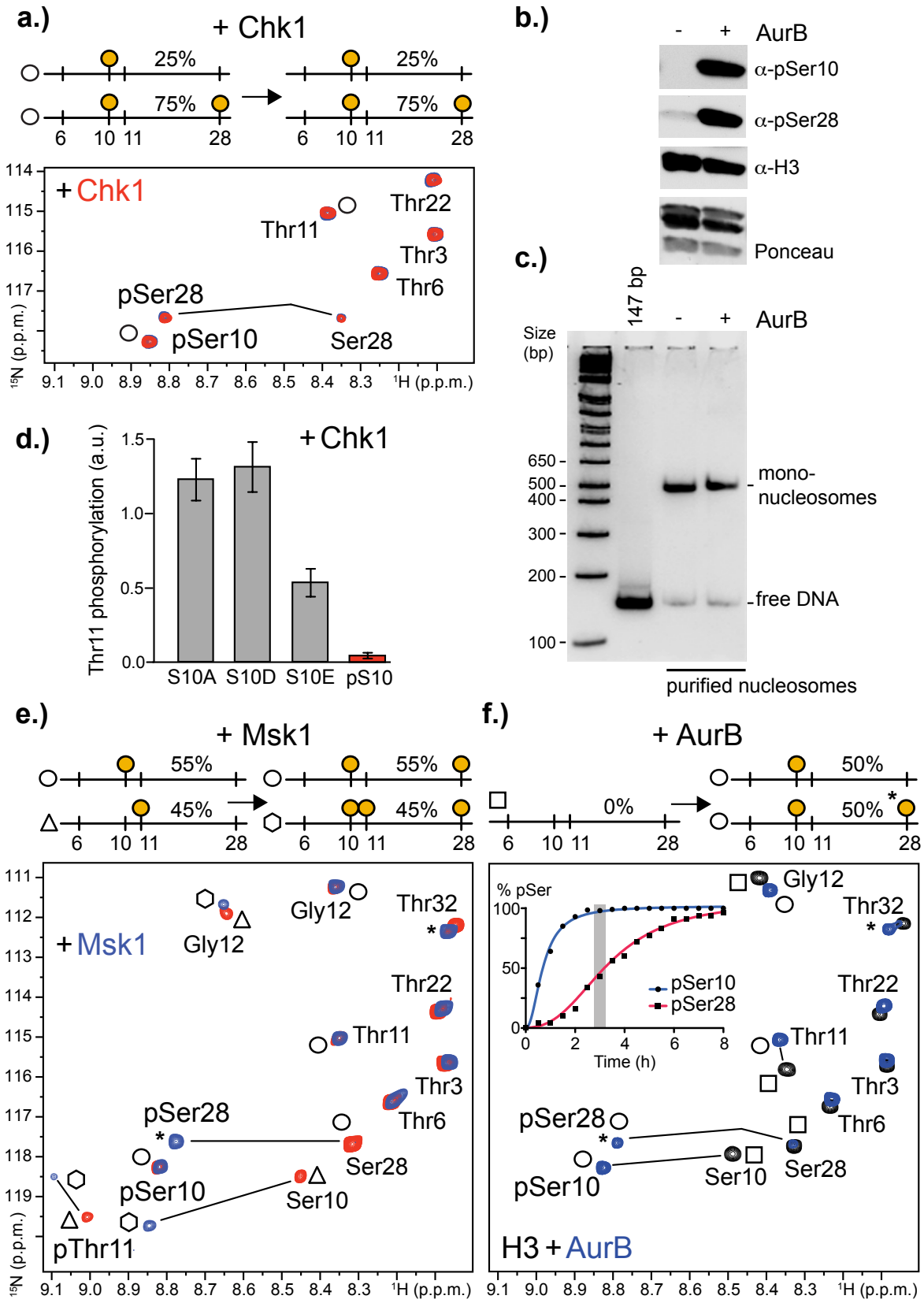

Supplementary Figure 1: *Histone H3 Ser10 phosphorylation cross-talk* (**a**) Superposition of 2D ^{1}H-^{15}N NMR spectra of AurB-modified H3 (*blue*) and upon incubation with Chk1 (*red*). Ser10 phosphorylation inhibits the subsequent, intramolecular modification of Thr11. (**b**) Preparation of unmodified and phospho-Ser10 Ser28 modified mono-nucleosomes (via reaction with AurB). (**c**) Native-PAGE analysis of nucleosome integrity after heat-inactivation of AurB. (**d**) Phospho-Thr11 levels in Chk1 reactions with uniform ^{15}N isotope-labeled H3 phospho-Ser10 and mutant Ser10 peptides (aa1-33), as determined by quantitative NMR phospho-signal integration. Relative reductions in Thr11 phosphorylation levels were determined. Error bars are STDs from two independent experiments. (**e**) Msk1 phosphorylates mixtures of phospho-Ser10 and phospho-Thr11 H3 peptides to yield double phospho-Ser10 Thr11 species. Ser28 phosphorylation is marked with an asterisk. (**f**) AurB modifies Ser10 and Ser28 in a stepwise manner (inset). Superposition of 2D ^{1}H-^{15}N NMR spectra of unmodified H3 (*black*) and AurB phosphorylated H3 (*blue*) obtained after 3 hours of kinase reaction at 295 K (grey bar in inset).

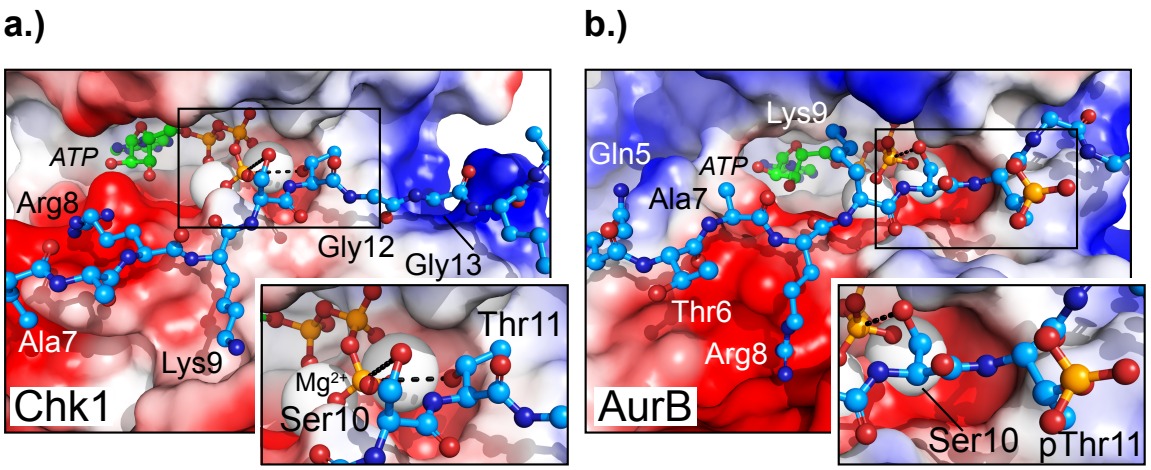

Supplementary Figure 2: *Models of Chk1 and AurB histone H3 kinase substrate complexes.* (**a**) X-ray structures of Chk1, AurB and PHKγt were used to create starting models for kinase bound histone H3 (see Supplementary Materials and Methods for details). Unmodified, phospho-Ser10 and phospho-Thr11 H3 Chk1 complexes were subjected to simulated annealing protocols. The consensus sequence for Chk1 substrates dictates an invariant Arg residue at the -3 position with respect to the canonical phosphorylation site. Initial starting structures of unmodified, phospho-Ser10 and phospho-Thr11 H3 Chk1 complexes, bound in a canonical and +1 register-shifted conformation, were generated *in silico* and subjected to simulated annealing. Phospho-Ser10 and phospho-Thr11 starting structures, irrespective of their kinase interaction register, rapidly dissociated from Chk1 during the initial steps of simulated annealing. The same was true for unmodified histone H3 initially bound in a +1 register-shifted conformation. The only starting structure for which an energy-minimized H3 Chk1 complex model was obtained is shown above. Electrostatic charge complementation of the invariant Chk1 consensus -3 position (i.e. Arg8) and an acidic patch of the catalytic kinase cleft is readily appreciated. In this model conformation, Thr11 is positioned as the canonical phospho-acceptor site, while Ser10 is in close proximity to kinase bound ATP (close-up view). Dual Thr11 and Ser10 phosphorylation may be accomplished in such a hypothetical conformation. In the +1 register-shifted conformation of the unmodified H3 Chk1 starting structure this interaction was not present. Instead, Ala7 was positioned above the acidic patch, Arg8 adopted the conformation previously occupied by Lys9 and Ser10 served as the canonical phospho-acceptor residue. Kinase dissociation of this register-shifted conformation may therefore be explained by lack of the aforementioned electrostatic substrate kinase interactions. In case of the phospho-Ser10 and phospho-Thr11 starting structures, strong interactions between the phosphate groups of Ser10 and Thr11 and Arg8 were observed during the initial steps of the simulated annealing protocol. These relieved the Arg8 interaction with the acidic kinase patch and resulted in rapid substrate dissociations from Chk1. While these simulations do not allow direct deductions of individual reaction mechanisms, the binding characteristics obtained *in silico* are in agreement with the experimentally observed phosphorylation behavior of Chk1, as described in the main text. (**b**) Simulated annealing routines were similarly performed for H3 AurB complexes. The consensus sequence for AurB substrates dictates an invariant Arg, or Lys residue at the -2 position with respect to the canonical phosphorylation site. Starting structures of unmodified and phospho-Thr11 H3 bound to AurB were generated. In contrast to the results obtained with Chk1, simulated annealing routines with both types of substrates produced stable, energy-minimized complex models. As shown above, the presence of phospho-Thr11 does not interfere with canonical Ser10 binding by AurB in the model.

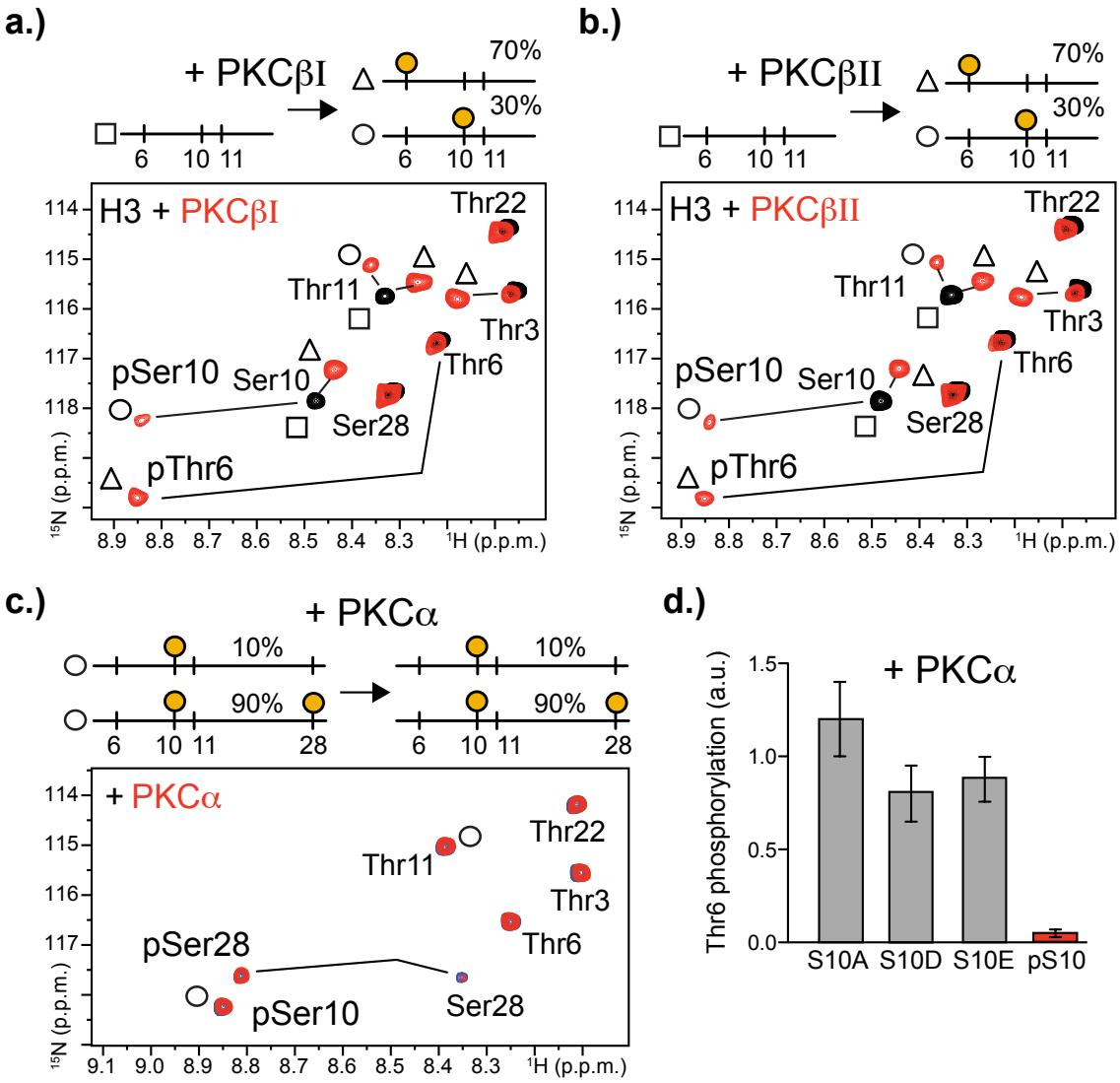

Supplementary Figure 3: *Histone H3 PKC phosphorylation.* (**a**) Superposition of 2D ^{1}H-^{15}N NMR spectra (selected region) of ^{15}N isotope-labeled H3 (*black*) and phosphorylated by PKCβI (*red*). Modification of Thr6 and Ser10 on different substrate molecules results in two sets of NMR signals that correspond to a superposition of individually modified H3 species. (**b**) Superposition of 2D ^{1}H-^{15}N NMR spectra of ^{15}N isotope-labeled H3 (*black*) and phosphorylated by PKCβII (*red*). (**c**) Superposition of 2D ^{1}H-^{15}N NMR spectra of ^{15}N isotope-labeled H3 substrate phosphorylated at Ser10 and Ser28 by AurB (*blue*) and after incubation with excess quantities of PKCα (*red*). Ser10 phosphorylation on all H3 substrate molecules inhibits the subsequent, intramolecular modification of Thr6 by PKCα. (**d**) Phospho-Thr6 levels in PKCα reactions with uniform ^{15}N isotope-labeled H3 phospho-Ser10 and Ser10 mutant peptides (aa1-33), as determined by quantitative NMR phospho-signal integration. Relative reductions in Thr6 phosphorylation levels were determined. Error bars are STDs from two independent experiments. Ser10 phosphorylation mimicking H3 mutations i.e. S10D and S10E fail to recapitulate the inhibitory potential of phospho-Ser10 peptides in PKCα modification reactions

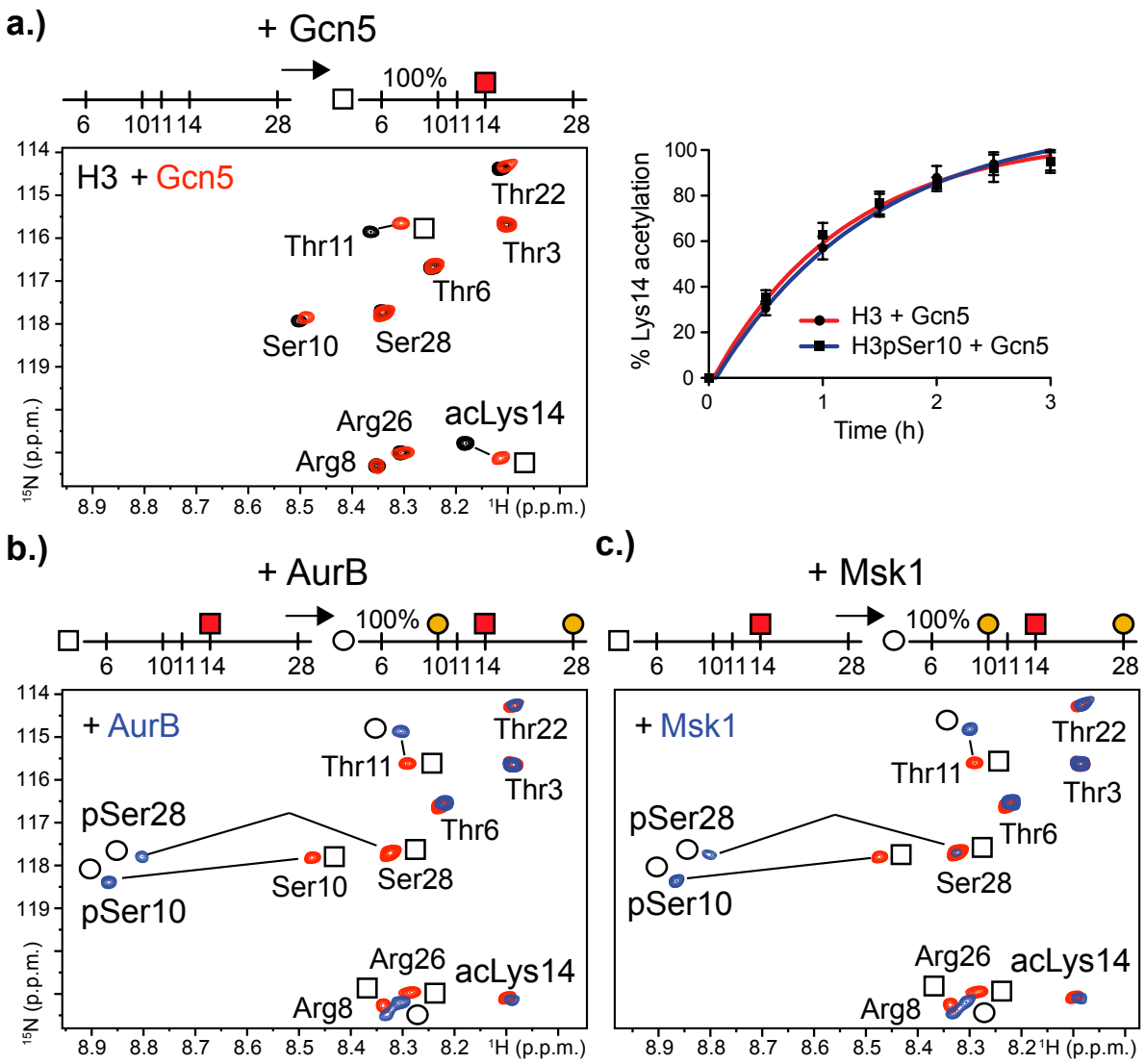

Supplementary Figure 4: *Histone H3 Lys14 acetylation behavior and influence on AurB and Msk1 H3 phosphorylation.* (**a**) Superposition of 2D ^{1}H-^{15}N NMR spectra (selected region) of ^{15}N isotope-labeled H3 (*black*) and upon Lys14 acetylation by full-length Gcn5 (*red*). The modification trajectory on the left depicts separately determined Lys14 acetylation rates of unmodified (*red*) and Ser10 phosphorylated H3 (*blue*, two independent NMR measurements). (**b**) Superposition of 2D ^{1}H-^{15}N NMR spectra of ^{15}N isotope-labeled H3 acetylated at Lys14 (*red*) upon reaction with AurB (*blue*), or (**c**) Msk1 (*blue*). Lys14 acetylation does not interfere with the phosphorylation behaviors of AurB i.e. phospho-Ser10 followed by phosphpho-Ser28, or Msk1 i.e. simultaneous modification of Ser10 and Ser28.

Supplementary Note

Synthetic H3 peptides (site-specific phosphorylated and non-phosphorylated) Human H3 peptides were synthesized using standard Fmoc-based solid-phase chemistry on an Intavis Respep XL synthesizer in a 25 μmol scale. TentaGel R RAM resin (cap.: 0,19 mmol/g) was used as a solid support and amino acid side-chains were protected as follows: Arg (Pbf), Cys (Trt), Lys(Boc), Gln(Trt), Ser(tBu) and Thr(tBu). Coupling reactions were performed with 2-(1H-benzotriazole-1-yl)-1,1,3,3-tetramethyluroniumhexafluorophosphate (HBTU) as the activation agent and N-Methylmorpholine (NMM) in DMF/NMP as base. Each successive amino acid was doubly coupled in 5-fold molar excess. Removal of the Fmoc groups was carried out with 20 % piperidine in DMF. All peptides (non-modified and specifically phosphorylated) contained an additional Cys residue at their C-termini. Phosphorylated building blocks were introduced manually using HBTU/N-Hydroxybenzotriazol (HOBt) and Diisopropylethylamine (DIPEA) in DMF. These reactions were performed in 4-fold molar excess for 2 h with a mixture of Fmoc-amino acid (100 μmol), HBTU (95 μmol), HOBt (95 μM) and DIPEA (150 μmol) in DMF followed by a capping step using Ac_2O and 2,6-Lutidine in DMF. Efficient synthesis required the installation of at least one pseudoproline dipeptide during synthesis. Peptides were cleaved from the resin with complete removal of the side-chain protection groups in a mixture of TFA/Phenol/Triisopropylsilane/H_2O (85:5:5:5) for 4 h. The cleaved products were precipitated in cold diethyl ether, centrifuged and washed with diethyl ether, dissolved in H_2O and lyophilized. Crude peptides were purified by preparative RP-HPLC and their expected molecular weights confirmed by mass spectrometry (MS). Standard amino acid derivatives were obtained from GLS (Shanghai, China). Coupling reagents were purchased from Iris

Nature Structural & Molecular Biology: doi:10.1038/nsmb.2310

Biotech (Marktredwitz, Germany). Phosphorylated building blocks and pseudoproline dipeptides were purchased from Merck Novabiochem (Darmstadt, Germany), Tentagel RAM resin from Rapp Polymere (Tübingen, Germany). All other chemicals were purchased from Sigma-Aldrich (Steinheim, Germany). Analytical and preparative RP-HPLC were performed on a Varian ProStar 210 HPLC system on either an analytical Nucleosil C18 column (5 μm, 4,6 x 250 mm, Machery-Nagel) or a preparative Dynamax C18 column (10 μm, 21,4 x 250 mm, Varian). Peptides were eluted with Solvents A (0,1% TFA in water) and B (80% ACN, 0,1% TFA in water) and a gradient of 5-95% B over 40 minutes. Peptides were analyzed by ESI-MS on a Mariner Biospectrometer Workstation 5240 and by analytical RP-HPLC.

Modeling of Chk1 and AurB complexes with N-terminal histone H3 substrates

Crystal coordinates of Chk1 and Aurora B were used as starting structures (pdb codes: 1IA8 and 2BFX). They were aligned to the crystal structure of PHKγt (pdb code: 2PHK) in order to obtain initial atom positions for ATP, two magnesium ions, bound water molecules and the backbone conformation of the H3 substrate. H3 side-chains were added and the resulting complexes were processed using the LEAP module of AMBER9 for adding hydrogen atoms, to charge neutralize the systems with chloride ions and to solvate in a TIP3P water box extending 12 Å from the complexes and to create the AMBER formatted input files. Simulated annealing routines were performed with the all-atom AMBER force field, the PARM99 parameters for proteins, polyphosphate parameters for ATP[1] and phospho-amino acid parameters for the modified H3 residues[2]. Calculations were carried out using the SANDER module, periodic boundary conditions and the particle-mesh Ewald (PME) approach with an 8 Å cutoff for non-bonded interactions. Water molecules were subjected to several

Nature Structural & Molecular Biology: doi:10.1038/nsmb.2310

rounds of initial minimizations (1500 cycles of steepest descent and 8500 steps of conjugate gradients). Equal numbers of cycles were used in all subsequent minimization steps. Energy minimizations were first performed for water and kinases with restrained ATP, magnesium and H3 peptide conformations, followed by minimizations of the entire systems. Simulated annealing protocols were performed as follows: Temperatures were raised from 0 K to 310 K over 35 ps by coupling the systems to heat baths with time constants of 0.5 ps and weak-coupling algorithms. Volumes were kept constant, pressures were adjusted by isotropic position scaling to 1 bar and water densities were set to 1.01 g cm^{-3} for two equilibration steps of 50 ps. The systems were then cooled from 310 K to 0 K over 35 ps and final rounds of energy minimizations were performed.

References

1. Meagher, K.L., Redman, L.T. & Carlson, H.A. Development of polyphosphate parameters for use with the AMBER force field. *J Comput Chem* **24**, 1016-25 (2003).
2. Homeyer, N., Horn, A.H., Lanig, H. & Sticht, H. AMBER force-field parameters for phosphorylated amino acids in different protonation states: phosphoserine, phosphothreonine, phosphotyrosine, and phosphohistidine. *J Mol Model* **12**, 281-9 (2006).

Nature Structural & Molecular Biology: doi:10.1038/nsmb.2310